Detectability of galactic supernova neutrinos coherently scattered on xenon nuclei in XMASS

K. Abe [a,d], K. Hiraide [a,d], K. Ichimura [a,d], Y. Kishimoto [a,d], K. Kobayashi [a,d], M. Kobayashi [a], S. Moriyama [a,d], K. Nakagawa [a], M. Nakahata [a,d], T. Norita [a], H. Ogawa [a,d], H. Sekiya [a,d], O. Takachio [a], A. Takeda [a,d], M. Yamashita [a,d], B.S. Yang [a,d], N.Y. Kim [b], Y.D. Kim [b], S. Tasaka [c,1], J. Liu [d,2], K. Martens [d], Y. Suzuki [d], R. Fujita [f], K. Hosokawa [f], K. Miuchi [f], N. Oka [f], Y. Onishi [f], Y. Takeuchi [f,d], Y.H. Kim [g,b], J.S. Lee [g], K.B. Lee [g], M.K. Lee [g], Y. Fukuda [h], Y. Itow [i,e], R. Kegasa [i], K. Kobayashi [i], K. Masuda [i], H. Takiya [i], H. Uchida [i], K. Nishijima [j], K. Fujii [k], I. Murayama [k], S. Nakamura [k], XMASS Collaboration [2,*]

[a] Kamioka Observatory, Institute for Cosmic Ray Research, University of Tokyo, Higashi-Mozumi, Kamioka, Hida, Gifu, 506-1205, Japan
[b] Center of Underground Physics, Institute for Basic Science, 70 Yuseong-daero 1689-gil, Yuseong-gu, Daejeon, 305-811, South Korea
[c] Information and multimedia center, Gifu University, Gifu 501-1193, Japan
[d] Kavli Institute for the Physics and Mathematics of the Universe (WPI), University of Tokyo, Kashiwa, Chiba, 277-8582, Japan
[e] Kobayashi-Maskawa Institute for the Origin of Particles and the Universe, Nagoya University, Furo-cho, Chikusa-ku, Nagoya, Aichi, 464-8602, Japan
[f] Department of Physics, Kobe University, Kobe, Hyogo 657-8501, Japan
[g] Korea Research Institute of Standards and Science, Daejeon 305-340, South Korea
[h] Department of Physics, Miyagi University of Education, Sendai, Miyagi 980-0845, Japan
[i] Institute for Space-Earth Environmental Research, Nagoya University, Nagoya, Aichi 464-8602, Japan
[j] Department of Physics, Tokai University, Hiratsuka, Kanagawa 259-1292, Japan
[k] Department of Physics, Faculty of Engineering, Yokohama National University, Yokohama, Kanagawa 240-8501, Japan

ABSTRACT

The coherent elastic neutrino-nucleus scattering (CEvNS) plays a crucial role at the final evolution of stars. The detection of it would be of importance in astroparticle physics. Among all available neutrino sources, galactic supernovae give the highest neutrino flux in the MeV range. Among all liquid xenon dark matter experiments, XMASS has the largest sensitive volume and light yield. The possibility to detect galactic supernova via the CEvNS-process on xenon nuclei in the current XMASS detector was investigated. The total number of events integrated in about 18 s after the explosion of a supernova 10 kpc away from the Earth was expected to be from 3.5 to 21.1, depending on the supernova model used to predict the neutrino flux, while the number of background events in the same time window was measured to be negligible. All lead to very high possibility to detect CEvNS experimentally for the first time utilizing the combination of galactic supernovae and the XMASS detector. In case of a supernova explosion as close as Betelgeuse, the total observable events can be more than $\sim 10^4$, making it possible to distinguish different supernova models by examining the evolution of neutrino event rate in XMASS.

© 2017 Elsevier B.V. All rights reserved.

1. Introduction

The neutral current interaction of neutrinos with nuclei,

$$\nu_\mu/\bar{\nu}_\mu + \text{nucleus} \rightarrow \nu_\mu/\bar{\nu}_\mu + \text{hadrons}, \tag{1}$$

was observed at the Gargamelle bubble chamber experiment at CERN in 1973 [1]. The energy of incident neutrinos was in the order of a few GeV. Freedman pointed out one year later [2,3] that a neutrino with an energy in the order of MeV could interact with all nucleons in a nucleus coherently,

$$\nu + \text{nucleus} \rightarrow \nu + \text{nucleus}, \tag{2}$$

resulting in a large cross section, approximately proportional to the square of the number of neutrons in the target nucleus. Given such

a large cross section, however, it has not been observed yet, primarily because the only observable of this interaction is the recoiled nucleus with its kinetic energy in the order of keV.

Although not yet observed, the coherent scattering has been believed to be the main mechanism for neutrinos to be trapped in the core of a supernova [4]. It has been proposed as a method to probe non-standard neutrino interactions with quarks, extra heavy neutral gauge bosons [5] and the neutron part of nuclear form factors [6]. A detector utilizing the coherent scattering was also proposed by Drukier and Stodolsky in 1984 [7] to detect neutrinos from spallation sources, reactors, supernovae, the Sun and the Earth, and by Goodman and Witten in 1985 [8] to detect some dark matter candidates. Among all available neutrino sources, galactic supernovae give the highest neutrino flux in the MeV range.

The coherent scattering has been listed as the primary physics goal of many experimental proposals, such as CoGeNT [9], TEX-ONO [10], NOSTOS [11], RED [12,13], CoSI [14], COHERENT [15], CENNS [16] and CONNIE [17] etc. In addition, experiments for low-energy solar neutrino, dark matter and neutrinoless double beta-decay have the potential to detect galactic supernova neutrinos coherently scattered on nuclei. Horowitz made a comprehensive comparison between different approaches [18]. He pointed out that the choice of the target nuclei involved a trade-off of many considerations. For example, heavy elements are preferred because of the large cross section, while light elements are preferred since they get more recoil energy, which relaxes the requirement on low energy threshold. And most importantly, the amount of target material should be as large as possible. Among all existing experiments, liquid xenon dark matter experiments seem to be the most practical choice for this purpose at this moment, given their large target masses, sufficiently low background and energy thresholds.

Most xenon based dark matter experiments utilize dual-phase time-projection chambers. Their potential to detect supernova neutrinos through the CEνNS channel is discussed in a recent paper [19] and references there in. The XMASS detector [20] located in the Kamioka Underground Observatory in Japan is a single-phase liquid-xenon scintillation detector. It contains the largest amount of liquid xenon and features the highest light yield among all running liquid-xenon dark-matter experiments. The high light yield ensures a sufficiently low energy threshold, while the background level around the threshold was measured to be negligible [21] in a 18 s time window, the typical time scale of a supernova neutrino burst. All make XMASS a promising experiment to detect supernova neutrinos through the coherent scattering channel. Neutrino-electron neutral current scatterings ($\nu + e^- \rightarrow \nu + e^-$) and neutrino-nucleus quasi-elastic scatterings are other possible observation channels. However, their cross sections are orders of magnitude smaller than that of coherent scatterings [22–27], and will not be discussed in this work.

Several detectors in the Kamioka Underground Observatory are capable of detecting supernova neutrinos along with many others in the world [28,29]. The water Čerenkov detector Super-Kamiokande can detect supernova neutrinos dominantly through the $\bar{\nu}_e + p \rightarrow e^+ + n$ channel [30,31]. Utilizing the neutral current interaction, XMASS is sensitive to all flavors of neutrinos. Another experiment, KamLAND, is also sensitive to all flavors through the neutrinos-proton elastic scattering [32,33] and excitation of carbon nuclei by neutrinos [34]. However, no information on the coherent scattering is given by KamLAND. The three experiments in Kamioka cover each other's dead time, are sensitive to different neutrino interactions and may provide comprehensive understanding of the supernova neutrino burst in case of a simultaneous observation.

The possibility to detect galactic supernova neutrinos coherently scattered with xenon nuclei in XMASS is calculated in this work. Since XMASS is a running detector with most of its properties having been studied systematically [20,21], the uncertainty of the estimation in the detection is minimized. However, the precision of such an estimation still suffers from the uncertainty in the theoretical prediction of supernova neutrino flux, as demonstrated recently by Chakraborty et al. [35].

In order to have a comprehensive understanding of the possible variation in the event rate predicted by various supernova models, the numeric database of supernova neutrino emission provided by Nakazato et al. [36] is used to calculate the coherent scattering event-rate in XMASS. Numeric results of a wide range of progenitors are provided including a black-hole-forming case. The canonical Livermore supernova model [30] is also used to calculate the event rate, the result of which can be used as a reference when compared to other estimations.

Two possible locations of galactic supernovae are assumed. One is 10 kpc away from the Earth, roughly at the center of the Milky Way. The other is 196 pc away from the Earth where Betelgeuse locates.

2. Coherent elastic neutrino-nucleus scattering

The differential cross section of the coherent scattering as a function of neutrino energy E_ν and nuclear recoil energy E_{nr} is taken from Ref. [5],

$$\frac{d\sigma}{dE_{nr}}(E_\nu, E_{nr}) = \frac{G_F^2 M}{2\pi} G_V^2 \left[1 + \left(1 - \frac{E_{nr}}{E_\nu} \right)^2 - \frac{ME_{nr}}{E_\nu^2} \right], \quad (3)$$

where G_F is the Fermi constant, M is target nuclear mass, and

$$G_V = [(\frac{1}{2} - 2\sin^2 \theta_W)Z - \frac{1}{2}N]F(q^2), \quad (4)$$

excluding non-standard neutrino interaction terms and neglecting the radiative corrections presented in Ref. [5]. The axial vector current leads to a small incoherent contribution to the total neutral current cross section and is ignored. The value of $\sin^2 \theta_W$ (θ_W is the weak mixing angle) is 0.23, taken from the Review of Particle Physics [37]. Z and N are the numbers of protons and neutrons in the nucleus, respectively. According to the definition in Ref. [3], the nuclear form factor $F(q^2)$ is the integral of the relative phase of the incident neutrino scattered by the nucleon at position $\mathbf{r}$:

$$F(q^2) = \int d\mathbf{r} e^{i\mathbf{q} \cdot \mathbf{r}} \rho(\mathbf{r}), \quad (5)$$

where $\rho(\mathbf{r})$ is the spatial density distribution of nucleons, normalized so that $\int d\mathbf{r}\rho(\mathbf{r}) = 1$. Helm proposed to reform it as $\rho(\mathbf{r}) = \int d\mathbf{r}' \rho_0(\mathbf{r}')\rho_1(\mathbf{r} - \mathbf{r}')$ [38], where ρ_0 represents a constant density inside a sphere with radius r_0, and ρ_1 a surface with thickness s. The form factor can then be expressed as [39]

$$F(q^2) = \frac{3j_1(qr_0)}{qr_0} e^{-\frac{1}{2}(qs)^2}, \quad (6)$$

where $j_1(qr_0) = [\sin(qr_0) - qr_0 \cos(qr_0)]/(qr_0)^2$ is the spheric Bessel function of the first order. The relation between nuclear radius r_n and r_0 [38–40] is $r_0^2 = r_n^2 - 5s^2$. Values of r_n are taken from Ref. [41] and listed in Table 1. The value of s is taken as 1 fm [39].

3. Core-collapse supernovae

Stars heavier than 8 $M_\odot$ end their lives as core-collapse supernovae. It is commonly believed that the shock wave losses its kinetic energy when propagating outward and stalls before blowing off the stellar envelope. Several mechanisms causing the shock wave to revive have been proposed [42–47]. Different models predict different shock wave revival times. Generally speaking, the

Table 1
Properties of natural xenon isotopes used in calculation.

Natural xenon isotope	Nuclear mass (GeV/c²)	Natural abundance (atomic %)	Nuclear radius (fm)
^{128}Xe	119.1147	1.92	4.776
^{129}Xe	120.0474	26.44	4.776
^{130}Xe	120.0777	4.08	4.783
^{131}Xe	121.9107	21.18	4.781
^{132}Xe	122.8413	26.89	4.787
^{134}Xe	124.7055	10.44	4.792
^{136}Xe	126.5702	8.87	4.799
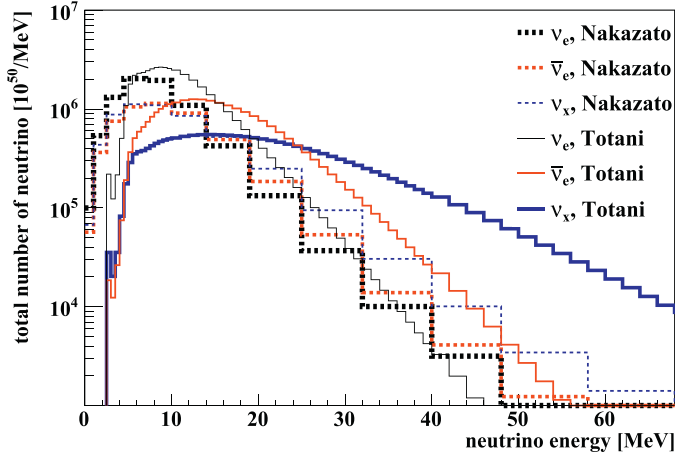
Fig. 1. Supernova neutrino energy-spectra integrated from the core collapse to about 18 s. Solid lines are the numeric results from Totani et al. [30]. Dashed lines are the numeric results from Nakazato et al. [36]. The parameters used to generate the spectra from Nakazato model are progenitor mass ($M_p = 20 \, M_\odot$), metalicity ($Z = 0.02$) and shock wave revival time ($t_{rev} = 200$ ms). ν_x represents neutrino flavors other than ν_e and $\bar{\nu}_e$.

later the revival, the more neutrinos are emitted because more material falls on to the acretion shock. This causes an uncertainty in the expected number of events observed in a detector. Nakazato et al. [36] proposed a simple method to manually combine their one dimensional simulations before and after the shock wave revival. The revival time t_{rev} is used as a parameter related to the yet unknown explosion mechanism. The number luminosity and energy spectrum of neutrinos as a function of time are provided by them in a publicly accessible database [48]. The results corresponding to $t_{rev} = 100, 200$ and 300 ms are provided in the current database. The influence of t_{rev} on the observed energy spectra and event rates can be investigated using those results. Other parameters that can be investigated using this database include the masses of supernova progenitors, M_p, ($M_p = 13, 20, 30$ and $50 \, M_\odot$ are provided) and the metalicity, Z, of the galaxy where those progenitors are located ($Z = 0.02$ and its 1/5 are provided). They are all used in this paper. The simulation result from Totani et al. published in 1998 [30] has been widely used in previous calculations. It is also used in this paper to provide a reference for comparison. Fig. 1 shows the neutrino energy spectra integrated from the core collapse till about 18 s later, provided by Totani et al. and Nakazato et al. The parameters used to generate the spectra from Nakazato model are $M_p = 20 \, M_\odot$, $Z = 0.02$ and $t_{rev} = 200$ ms. The total energy carried by neutrinos in this model is 1.92×10^{53} erg. The average energies of different neutrino flavors given by this model are 9.32 MeV, 11.1 MeV and 11.9 MeV for ν_e, $\bar{\nu}_e$ and ν_x, respectively. The energy release as a function of the three input parameters is summarized in Table 1. in reference [36].

4. XMASS detector

The key factors for a successful detection of galactic supernova neutrinos coherently scattered in a detector include large target mass, low energy threshold and low background. All of them are fulfilled in the current XMASS detector [20]. It is a liquid-xenon scintillator-detector, and the scintillation light is collected by 642 photomultiplier tubes (PMTs) mounted on a pentakis-dodecahedral support structure with a diameter of about 80 cm. The active region contains $M_{det} = 832$ kg of liquid xenon, the largest among all liquid xenon dark matter experiments. The photocathode coverage of the inner surface of the detector is 62.4%. A global trigger is generated if the number of hit PMTs within a 200 ns window is above three. The detector is located underground in the Kamioka Observatory at a depth of 2700 meter-water-equivalent. The cosmic ray induced background is sufficiently suppressed. To shield the scintillator volume from external gammas, neutrons, and muon-induced backgrounds, the copper vessel is placed at the center of a cylindrical tank filled with pure water with a diameter of 10 m and a height of 11 m. This volume is viewed by 72 Hamamatsu R3600 20-inch PMTs to provide both an active muon veto and passive shielding against these backgrounds. The background level around the threshold was measured in the commissioning runs [21]. XMASS started the physics run in November 2013 after the detector refurbishment and the background rate is further reduced [49] to be negligible in a 18 s time window, the typical time scale of a supernova neutrino burst. This makes it possible to utilize all sensitive volume of XMASS for supernova neutrino detection.

5. Energy spectra of supernova neutrino events

The differential event rate of supernova neutrinos in the liquid xenon target in XMASS as a function of the true nuclear recoil energy E_{nr} can be expressed as:

$$\frac{dR_0}{dE_{nr}}(E_{nr}) = \frac{M_{det}N_A}{A(4\pi d^2)} \sum_{i=\nu_e, \bar{\nu}_e, \nu_x} \int_{E_{min}}^{\infty} \frac{d\sigma}{dE_{nr}}(E_\nu, E_{nr}) f_i(E_\nu) dE_\nu, \quad (7)$$

where N_A is the Avogadro's number, A is the averaged atomic mass of natural xenon and d is the distance between the supernova and the detector, $E_{min} = (E_{nr} + \sqrt{E_{nr}^2 + 2ME_{nr}})/2$ is the minimum energy a neutrino must have in order to give to the nucleus a recoil energy E_{nr}, and $f_i(E_\nu)$ is the neutrino energy spectra shown in Fig. 1.

The upper most curve in Fig. 2 shows the true recoil energy spectrum calculated with Eq. (7) above 1 keV. Nuclear recoils below 1 keV create less than 1 photoelectron assuming standard liquid xenon scintillation efficiency [50] and the light yield recorded in XMASS [20], hence are ignored.

The full XMASS Monte Carlo simulation is used to estimate the detection efficiency $\varepsilon(E_{nr})$. The upper most curve in Fig. 2 is used to sample the recoil energies of xenon nuclei as input for this Geant4-based simulation. The quenching of nuclear recoil energy in the scintillation process, the optical properties of liquid xenon, copper and PMTs, the quantum efficiency of PMTs and the electronic smearing of the number of photoelectrons are all implemented [20] in addition to the tracking process provided by Geant4. A PMT with the number of photoelectrons above 0.25 is recorded as a hit. The total number of hits, N_{hits}, is recorded for each simulated event. The detection efficiency $\varepsilon(E_{nr})$ is defined as the fraction of events with $N_{hits} > 3$ at a certain recoil energy E_{nr}. The realistic recoil energy spectrum is then

$$\frac{dR}{dE_{nr}}(E_{nr}) = \varepsilon(E_{nr}) \times \frac{dR_0}{dE_{nr}}(E_{nr}) \quad (8)$$

as shown in the middle curve in Fig. 2.
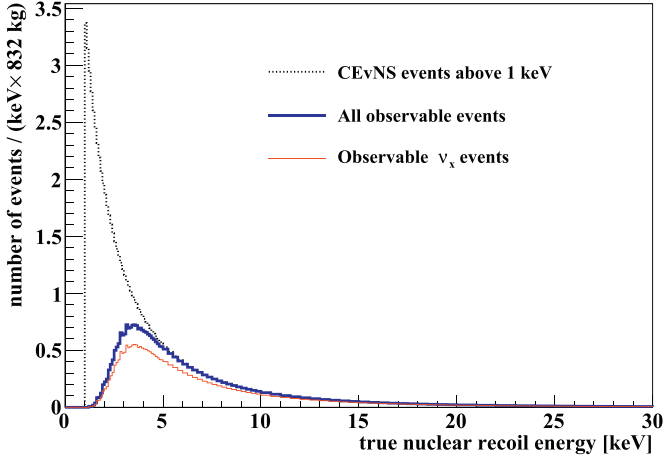
Fig. 2. Energy spectrum as a function of true xenon nuclear recoil energy. The upper most and middle curves are the energy spectra with and without taking into account the detection efficiency, respectively. The lower most curve shows the contribution from ν_x only. The upper line is calculated above 1 keV. The supernova model used here is the one from Nakazato et al. with $M_p = 20\ M_\odot, Z = 0.02$ and $t_{rev} = 200$ ms. This specific model predicts neither most nor least neutrino flux, hence is chosen to create the plot in order to avoid any visual bias. The distance of the supernova from the Earth is assumed to be 10 kpc.
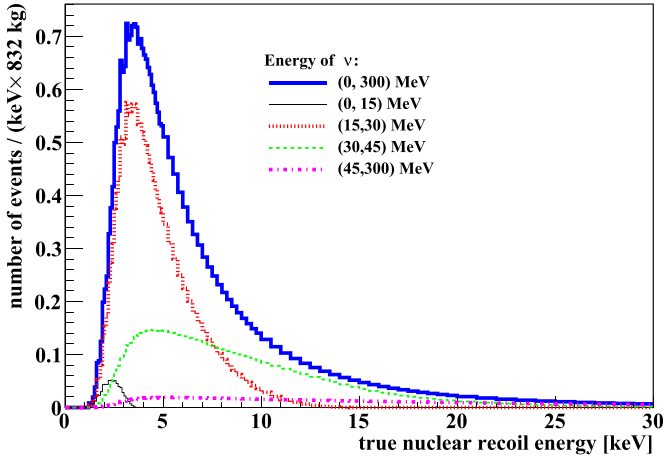
Fig. 3. Sensitivity to various supernova neutrino energy regions. The upper most curve is exactly the same as the middle curve in Fig. 2.

The lower most curve in Fig. 2 shows the contribution to the observable energy spectrum from ν_x only. Clearly, XMASS detects mostly ν_x. The upper most curve in Fig. 3 is exactly the same as the middle curve in Fig. 2. The lower curves in Fig. 3 show contributions from neutrinos in various energy regions. Due to the threshold effect, XMASS is mostly sensitive to neutrinos above ~ 15 MeV from the tail parts of the supernova neutrino spectra shown in Fig. 1.

The total number of observable events, N_{obs}, can be obtained by integrating the realistic energy spectrum:

$$N_{obs} = \int \frac{dR}{dE_{nr}}(E_{nr})dE_{nr} \qquad (9)$$

Practically, it is enough to integrate over $E_{nr} = 1\text{--}50$ keV as seen in the middle curve of Fig. 2. The values of N_{obs} from different supernova models are listed in Table 2. Two distances are chosen for comparison, $d = 10$ kpc is roughly the distance from the center of the Milky Way to the Earth, $d = 196$ pc is the distance from Betelgeuse to the Earth. The number of observable events predicted by most of the Nakazato models are significantly less than that predicted by the Livermore model. However, one Nakazato model,

Table 2
Number of observable supernova events in XMASS. The weakest Nakazato model is the one with $M_p = 20\ M_\odot$, $Z = 0.02$ and $t_{rev} = 100$ ms. The brightest Nakazato model is the one with $M_p = 30\ M_\odot$, $Z = 0.02$ and $t_{rev} = 300$ ms. The black-hole-forming model is the one with $M_p = 30\ M_\odot, Z = 0.004$. Neutrino energy spectra used in the calculation are all integrated from core collapse till about 18 s later.

| Supernova model	$d = 10$ kpc	$d = 196$ pc
Livermore	15.2	3.9×10^4
Nakazato (weakest)	3.5	0.9×10^4
Nakazato (brightest)	8.7	2.3×10^4
Nakazato (black hole)	21.1	5.5×10^4
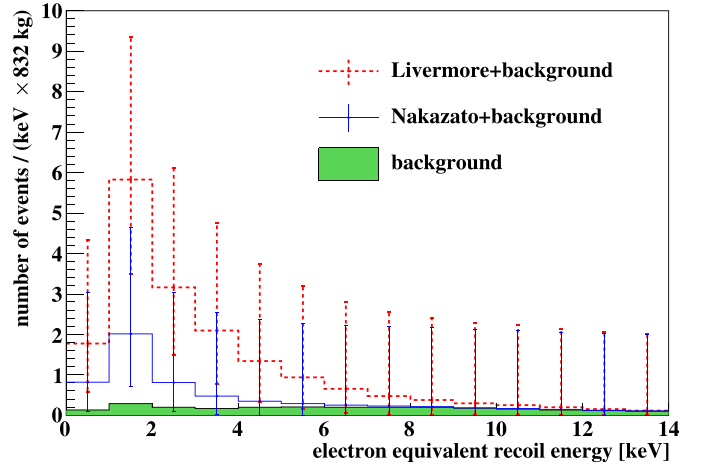
Fig. 4. The solid histogram in the middle is the same recoil energy spectrum as the middle curve of Fig. 2, but in the unit of *electron equivalent* instead of the *true nuclear recoil* energy. The dashed red histogram on the top is the *electron equivalent* recoil energy spectrum of the Livermore model. Both of them are draw on top of the expected background estimated from XMASS measurements, shown as the filled green histogram on the bottom.

which forms a black-hole, predicts similar number of observable events as the Livermore model. This points out the possibility to detect failed supernovae with no optical signal. In case of a supernova as close as Betelgeuse, all the models predict a definitely possible observation.

The energy of an event in XMASS is estimated by converting the recorded number of photoelectrons to keV using a measured relationship between these two. Such a relationship is obtained in energy calibrations at various locations in the detector using γ or X-ray sources with different energies as detailed in reference [20]. There is less than 10% difference in the energy converted this way from events with the same number of photoelectrons but at different locations [51]. Due to the fact that the scintillation efficiencies of nuclear and electronic recoil events are different [50], the energy calibrated this way is called explicitly *electron equivalent* energy to avoid ambiguity. The energy resolution is 36% at 1 keV (electron equivalent), dominated by Poisson statistics [51].

The solid histogram in the middle of Fig. 4 shows the same recoil energy distribution as the middle curve of Fig. 2, but in the unit of *electron equivalent* recoil energy instead of the *true nuclear recoil* energy. It is converted from the distribution of number of photoelectrons obtained from the full XMASS simulation. The spectrum is plotted on top of the expected background spectrum estimated from XMASS measurements, shown as the filled histogram on the bottom of Fig. 4. The error bars represent Poisson 68% CL intervals. The error bars in the background spectrum are invisibly small. For comparison, the *electron equivalent* recoil energy spectrum of the Livermore model is generated the same way and shown as the dashed histogram on the top of Fig. 4.
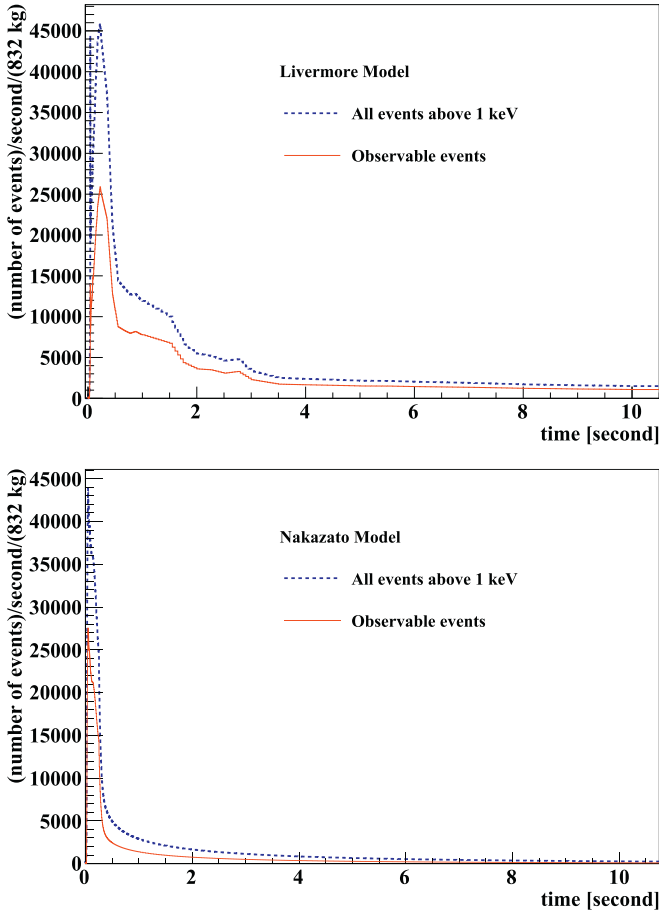
Fig. 5. Rate of CEvNS events in XMASS for a supernova 196 pc away from the Earth predicted by the Livermore model (upper plot) and the Nakazato model with $M_p = 20$ M$_\odot$, $Z = 0.02$ and $t_{rev} = 200$ ms (lower plot). This specific Nakazato model predicts neither most nor lest neutrino flux, hence is chosen to create the plot in order to avoid any visual bias. The upper lines correspond to all the CEvNS events above 1 keV nuclear recoil energy predicted by models; the lower lines corresponds to all events that can be detected in XMASS. About half of the events are detectable.

6. Event rate

As shown in Table 2, the average event rate in XMASS can be as high as a few thousand events per second for a supernova as close as Betelgeuse. Given such a high rate, it is possible to study in detail the supernova explosion mechanism by examining the time evolution of the event rate, since the flux and energy of the neutrinos predicted by different models vary in different phases of the explosion. Fig. 5 shows the rate of CEvNS events in XMASS for a supernova 196 pc away from the Earth predicted by the Livermore model and Nakazato model with $M_p = 20$ M$_\odot$, $Z = 0.02$ and $t_{rev} = 200$ ms, assuming without any DAQ loss. Different supernova models can be clearly distinguished.

Event rates of other neutrino interactions such as neutrino-electron neutral current scatterings and neutrino-nucleus quasi-elastic scatterings are not negligible in this case. Possible optimization of XMASS electronic system is under investigation to cope with such a high event rate.

7. Conclusion

The possibility to detect galactic supernova neutrinos coherently scattered with xenon nuclei in XMASS was examined in detail. The predicted number of observed events depend on two factors, one is the detection efficiency of the detector at low nuclear recoil energy, the other is the neutrino flux predicted by the supernova model used for the calculation. The former is estimated using full XMASS simulation. The latter is estimated by examining all models available in Nakazato's database [36]. The predicted number of observable events in XMASS ranges from 3.5 to 21.1 for a supernova in the center of the Milky Way, while the number of background events in the same time and energy window is observed to be negligible. It is hence possible for XMASS to experimentally observe galactic supernova neutrinos coherently scattered on xenon nuclei for the first time. In case of a supernova as close as Betelgeuse, the average event rate is above thousands per second, making it possible to distinguish between different supernova models by examining the time evolution of the event rate. Such a detection would provide not only the experimental evidence of CEvNS, but also comprehensive information about the supernova explosion mechanism.

References

[1] F. Hasert, et al., Phys. Lett. B 46 (1973) 138.
[2] D.Z. Freedman, Phys. Rev. D 9 (1974) 1389.
[3] D.Z. Freedman, et al., Ann. Rev. Nucl. Part. Sci. 27 (1977) 167.
[4] H.-T. Janka, et al., Phys. Rep. 442 (2007) 38.
[5] J. Barranco, et al., JHEP 12 (2005) 21.
[6] K. Patton, et al., Phys. Rev. C 86 (2012) 024612.
[7] A. Drukier, L. Stodolsky, Phys. Rev. D 30 (1984) 2295.
[8] M.W. Goodman, E. Witten, Phys. Rev. D 31 (1985) 3059.
[9] P.S. Barbeau, et al., J. Cosmo. Astropart. Phys. 2007 (2007) 9.
[10] H.T. Wong, Mod. Phys. Lett. A 23 (2008) 1431.
[11] I. Giomataris, et al., JINST 3 (2008) P09007.
[12] D.Y. Akimov, et al., JINST 8 (2013) P10023.
[13] D.Y. Akimov, et al., J. Phys. 675 (1) (2016) 012016.
[14] J. Collar, N. Fields, M. Hai, T. Hossbach, J. Orrell, C. Overman, G. Perumpilly, B. Scholz, Nucl. Instrum. Meth. A 773 (2015) 56–65.
[15] D. Akimov, et al., arXiv: 1509.08702 (2015).
[16] S. Brice, et al., Phys. Rev. D 89 (7) (2014) 072004.
[17] A. Aguilar-Arevalo, et al., JINST 11 (2016) P07024.
[18] C. Horowitz, et al., Phys. Rev. D 68 (2003) 023005.
[19] R.F. Lang, et al., Phys. Rev. D 94 (10) (2016) 103009.
[20] K. Abe, et al., Nucl. Instr. Meth. A 716 (2013) 78.
[21] K. Abe, et al., Phys. Lett. B 719 (2013) 78.
[22] W. Marciano, Z. Parsa, J. Phys. G Nucl. Part. Phys. 29 (2003) 2629.
[23] V. Chasioti, T. Kosmas, Nucl. Phys. A 829 (2009) 234.
[24] E. Ydrefors, et al., Nucl. Phys. A 896 (2012) 1.
[25] P.C. Divari, Adv. High Energy Phys. 2012 (2012) 1.
[26] W. Almosly, et al., J. Phys. G Nucl. Part. Phys. 40 (2013) 095201.
[27] P.C. Divari, Adv. High Energy Phys. 2013 (2013) 1.
[28] K. Scholberg, Ann. Rev. Nucl. Part. Sci. 62 (1) (2012) 81–103.
[29] A. Mirizzi, et al., Riv. Nuovo Cim. 39 (2016) 1.
[30] T. Totani, et al., Astrophys. J. 496 (1998) 216.
[31] M. Ikeda, et al., Astrophys. J. 669 (2007) 519–524.
[32] J.F. Beacom, et al., Phys. Rev. D 66 (2002) 33001.
[33] B. Dasgupta, J.F. Beacom, Phys. Rev. D 83 (11) (2011) 113006.
[34] A. Gando, et al., Astrophys. J. 745 (2012) 193.
[35] S. Chakraborty, et al., Phys. Rev. D 89 (2014) 013011.
[36] K. Nakazato, et al., Astrophys. J. Suppl. Ser. 205 (2013) 2.
[37] K. Olive, et al., Chin. Phys. C 38 (2014) 090001.
[38] R. Helm, Phys. Rev. 104 (1956) 1466.
[39] J. Engel, Phys. Let. B 264 (1991) 114.
[40] J.D. Lewin, P.F. Smith, Astropart. Phys. 6 (1996) 87.
[41] G. Fricke, et al., Atom. Dat. Nucl. Data. Tab. 60 (1995) 117.
[42] J.R. Wilson, Num. Astrophys. Proc. Symp. (1985) 422. in honour of James R.Wilson

[43] H.A. Bethe, J.R. Wilson, Astrophys. J. 295 (1985) 14.
[44] H.A. Bethe, Rev. Mod. Phys. 62 (1990) 801.
[45] A. Burrows, et al., Astrophys. J. 640 (2006) 878.
[46] T. Fischer, et al., Astrophys. J. Suppl. Ser. 194 (2011) 39.
[47] K. Kotake, et al., Rep. Prog. Phys. 69 (2006) 971.
[48] http://asphwww.ph.noda.tus.ac.jp/snn/, 2013.
[49] K. Hiraide, et al. (2015). ArXiv:1506.08939.
[50] L. Baudis, et al., Phys. Rev. D 87 (2013) 115015.
[51] K. Abe, et al., Phys. Lett. B 759 (2016) 272.